

# Europium-Doped Yttrium Silicate Nanophosphors Prepared by Flame Synthesis

X. Qin<sup>\*</sup>, Y. Ju<sup>\*\*</sup>, S. Bernhard<sup>\*\*\*</sup> and N. Yao<sup>\*\*\*\*</sup>

<sup>\*</sup>Princeton University, Princeton, NJ, USA, xqin@princeton.edu

<sup>\*\*</sup>Princeton University, Princeton, NJ, USA, yju@princeton.edu

<sup>\*\*\*</sup>Princeton University, Princeton, NJ, USA, sbernhar@princeton.edu

<sup>\*\*\*\*</sup>PRISM, Princeton University, Princeton, NJ, USA, nyao@princeton.edu

## ABSTRACT

Europium doped yttrium silicate nanophosphors were successfully synthesized for the first time by using the flame spray pyrolysis method. The effect of silicon concentration on the crystal structure, morphology, and photoluminescence intensity of the  $Y_2SiO_5:Eu$  phosphors were investigated. The as-prepared nanophosphors give good red luminescence under ultraviolet excitation compared with commercial  $Y_2O_3:Eu$  lamp phosphors, and have spherical morphology and narrow size distribution. The crystal structure and photoluminescence intensity were strongly affected by the ratio of silicon to yttrium in the precursor solution. The maximum photoluminescence intensity obtained from the phosphors prepared from silicon to yttrium ratio of 1.25. A concentration quenching limit was observed at 30 mol% Eu of yttrium component. The flame spray pyrolysis demonstrated advantages over other synthesis methods for the preparation of  $Y_2SiO_5:Eu$  nanophosphors and the potential for industrial applications.

**Keywords:** yttrium silicate, europium-doped, flame synthesis, nanophosphors, photoluminescence.

## 1 INTRODUCTION

Yttrium silicate ( $Y_2SiO_5$ ) is an important luminescent host material for various rare-earth activators [1]. Its high chemical stability makes it a good laser host [2,3].  $Tb^{3+}$  and  $Ce^{3+}$  doped yttrium silicates are efficient green and blue phosphors, respectively [4,5].  $Y_2SiO_5:Eu^{3+}$  has a sharp emission in red and is a promising phosphor for high resolution displays [6]. Moreover,  $Y_2SiO_5:Eu^{3+}$  was also found to be a promising candidate for coherent time-domain optical memory applications [7]. Recently, the study of europium doped yttrium silicate attracts new attention because of the applications in homeland security.

There are two types of monoclinic  $Y_2SiO_5$  crystal:  $X_1$ - and  $X_2$ -type [8]. The  $X_1$ - and  $X_2$ -types can be formed by changing the synthesis temperature. The high-temperature synthesis leads to the  $X_2$ -type and low-temperature synthesis to the  $X_1$ -type [9]. In general, the rare-earth doped yttrium silicate phosphors have been mainly prepared by the solid-state reaction of  $Y_2O_3$ ,  $SiO_2$  and activators at high temperature [4, 10]. However, this technique requires a long processing time, repeated milling, and washing with

chemicals, and thus yields a concern of purity. In addition, these processes tend to degrade the luminescence properties and yield irregularly shaped particles. The sol-gel technique has also been employed to synthesize  $Y_2SiO_5$  by some researchers [10, 11, 12, 13]. The as-prepared powders obtained from the sol-gel method have low crystallinity and require post-treatment at high temperature to crystallize. Spray pyrolysis was also used to prepare  $Y_2SiO_5:Ce$  [5] and  $Y_2SiO_5:Tb$  [14] particles possessing a spherical morphology. However, spray pyrolysis has a problem of formation of hollow and porous particles which are not desirable for the luminescence of phosphors.

In our recent work, a flame spray pyrolysis technique was successfully applied for the synthesis of yttria nanophosphors doped with europium [15]. The use of combustion can avoid hollowness and provide the high temperature environment which is favorable to phosphor synthesis. The flame temperature and particle residence time, which are very important parameters determining particle characteristics, can be easily controlled by varying fuel and oxidizer flow rates. Despite of the merits of flame synthesis, however, there have been no reports available on the flame synthesis of  $Y_2SiO_5:Eu^{3+}$  nanophosphors and the relation between the flame properties and nanophosphor properties has not been well understood. The objective of this work was to utilize the flame synthesis method for the preparation of  $Y_2SiO_5:Eu^{3+}$  nanophosphors.

## 2 EXPERIMENTAL

The details of the flame spray pyrolysis system used in this work are given our previous study of  $Y_2O_3:Eu^{3+}$  [15]. The system consisted of a spray generator, a coflow burner, a quartz reactor, particle collection filters and a vacuum pump. An ultrasonic spray generator operating at 1.7 MHz was used to generate fine spray droplets which were then carried into the flame by nitrogen gas through a central tube. The flame nozzle consisted of three concentric stainless steel tubes. A methane and oxygen nonpremixed flame was used for the flame synthesis. An air coflow was also introduced into the reactor to control the particle residence time. The starting materials of tetraethyl orthosilicate [ $TEOS$ ,  $(C_2H_5O)_4Si$ , 99.9%, Alfa Aesar], yttrium nitrate [ $Y(NO_3)_3 \cdot 6H_2O$ , 99.9%, Alfa Aesar] and europium nitrate [ $Eu(NO_3)_3 \cdot 6H_2O$ , 99.9%, Alfa Aesar] were dissolved in ethyl alcohol. The overall concentration of the precursor solution was varied from 0.001 to 0.1 M to obtain

different sized particles. The europium doping concentration (represented by  $x$ , which is the mole fraction of Eu in the formulae  $Y_{2-x}Eu_xSiO_5$ ) was varied from 0.1 to 0.7 (or 5 mol % to 35 mol % Eu of Y).

The particles were collected using a micron glassfiber filter (Whatmann GF/F) located 30 cm above the flame. Powder X-ray diffractometry (XRD, 30 kV and 20 mA,  $CuK\alpha$ , Rigaku Miniflex) was used for crystal phase identification and estimation of the crystalline size. The particle powders were pasted on a quartz glass and the scan were conducted in the range of  $10^\circ$  to  $60^\circ$  ( $2\theta$ ). The morphology and size of particles was examined using a field-emission scanning electron microscope (FE-SEM, Philips XL30). The photoluminescence spectra of the samples were measured with a Jobin-Yvon Fluorolog-3 fluorometer equipped with a front face detection setup and two double monochromators. The samples were excited with a 150 W Xenon lamp and a 2 nm slit width was used for both monochromators. All samples were examined at room temperature at 298 K.

### 3 RESULTS AND DISCUSSION

The crystal structure of the as-prepared and post-treated europium-doped yttrium silicate phosphors was examined by X-ray diffractometry. The effect of silicon (TEOS) concentration with respect to yttrium on the crystal phase of  $Y_2SiO_5:Eu^{3+}$  was investigated. Figure 1 shows the XRD spectra of the  $Y_2SiO_5:Eu^{3+}$  particles at different ratio of TEOS to yttrium, which is defined as the equivalence ratio,  $\phi = (X_{TEOS}/X_Y) / (X_{TEOS}/X_Y)_{stoi}$ , where  $X$  is the mole fraction. The particles were synthesized from stoichiometric TEOS ( $\phi = 1$ ) and rich TEOS ( $\phi > 1$ ) conditions. It is seen in Fig.1 that depending on the equivalence ratio of TEOS, there are three different crystalline phases. For TEOS equivalence ratio below 1.25, the XRD spectra (cf. Fig.1a) shows that flame synthesis results in an incomplete crystalline phase of  $X_1-Y_2SiO_5$ . Comparing with the spectrum data of JCPDS card 21-1456 [16] (indicated by ■ marks in Fig. 1b), many small peaks cannot be observed in Fig. 1a. This incomplete phase occurs because of the loss of silicon (TEOS) in the preheating zone of the flame. Because the boiling point of TEOS is low ( $165^\circ C$ ), a significant portion of TEOS evaporate in the preheating zone before pyrolysis. Therefore, in the flame zone, the TEOS equivalence ratio is less than unity. As a result, the particles prepared from the stoichiometric solution of TEOS and yttrium nitrate had small peaks corresponding to  $Y_2O_3$  existing as an impurity.

When the TEOS equivalence ratio was increased to  $\phi = 1.25$ , the XRD spectra shows that the pure phase of  $Y_2SiO_5$  was obtained (Fig. 1b). As mentioned previously,  $Y_2SiO_5$  is polymorphic and crystallizes in the monoclinic  $X_1$ - or  $X_2$ -type at different synthesis temperature. The XRD spectra in Figs. 1b and 1c show that the as-prepared  $Y_2SiO_5:Eu^{3+}$  phosphors have an  $X_1$ -type crystal structure, which was confirmed by comparing with the diffraction data of JCPDS

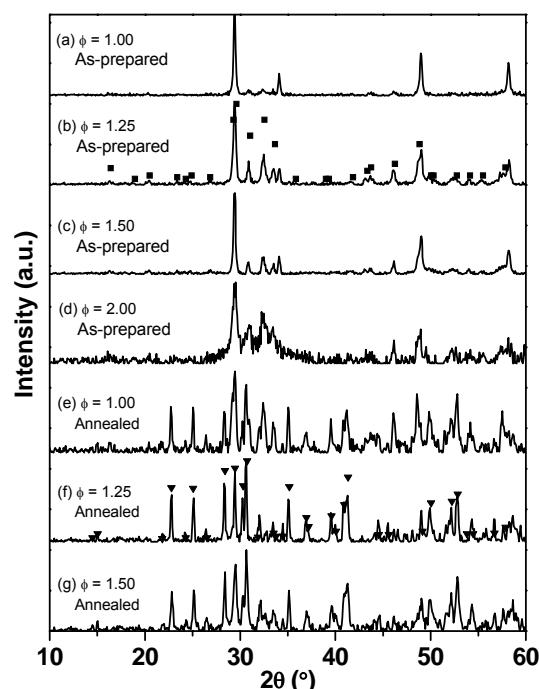


Figure 1: XRD spectra of  $Y_{1.9}Eu_{0.1}SiO_5$  particles prepared from different equivalence ratios: (a)  $\phi=1.0$ , as-prepared; (b)  $\phi=1.25$ , as-prepared; (c)  $\phi=1.50$ , as-prepared; (d)  $\phi=2.0$ , as-prepared; (e)  $\phi=1.00$ , annealed; (f)  $\phi=1.25$ , annealed; (g)  $\phi=1.50$ , annealed at  $1300^\circ C$  for 3 hr. The ■ mark in (b) indicates the diffraction data of  $X_1-Y_2SiO_5$  from JCPDS card 21-1456. The ▼ mark in (f) indicates the diffraction data of  $X_2-Y_2SiO_5$  from JCPDS card 21-1458.

card 21-1456 (indicated by ■ marks in Fig. 1b). These results show that the flame synthesis method of  $Y_2SiO_5:Eu^{3+}$  phosphors has a great advantage over the other synthesis methods. The as-prepared  $X_1-Y_2SiO_5:Eu^{3+}$  particles from flame synthesis have a strong fluorescence and require no additional post heat treatment. As reported from previous studies (sol-gel [13], spray pyrolysis [14], etc.), the as-prepared particles from these methods exhibit poor crystalline structure and fluorescent properties because of the amorphous structure due to the low synthesis temperature, and heat treatment up to  $1200^\circ C$  is necessary for  $X_1$ -type phase. As the TEOS equivalence ratio further increases ( $\phi \geq 2.0$ ), the results showed that the particles are dominated by the  $SiO_2$  amorphous structures and the XRD spectra (cf. Fig. 1d) of  $X_1$ -type phase becomes much weak. Therefore, the ratio of TEOS to yttrium in the precursor solution has a significant impact on the crystal phase of the phosphors. In addition, Figs.1e-1g shows that after annealing the as-prepared particles at  $1300^\circ C$  for 3 hours, the  $X_1-Y_2SiO_5:Eu^{3+}$  particles transformed to  $X_2$ -type. The ▼ marks in Fig. 1f represent the diffraction data of JCPDS card 21-1458 [17], which is  $X_2-Y_2SiO_5$ .

Figure 2 shows the scanning electron micrographs of the as-prepared  $Y_2SiO_5:Eu^{3+}$  particles at different ratios of silicon to yttrium, europium doping concentration and overall precursor concentration. There is little effect on the

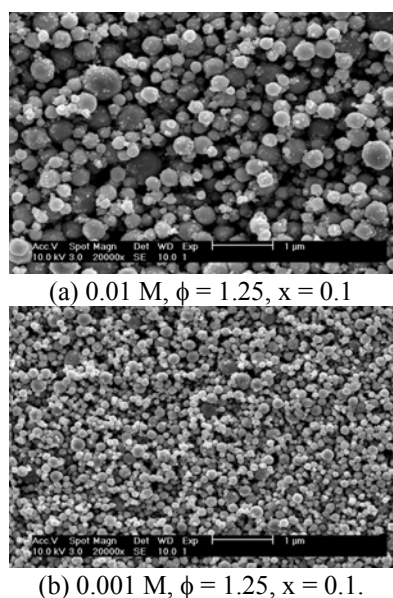


Figure 2: PL spectra of  $X_1$ - $Y_{2-x}Eu_xSiO_5$  ( $x = 0.1$ ) particles from different TEOS concentration.

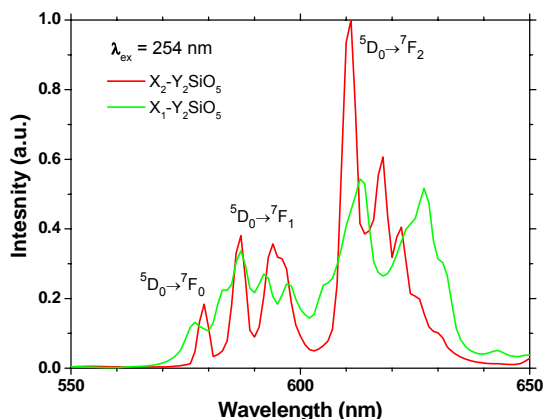


Figure 3: PL spectra of  $X_1$ -type (as-prepared) and  $X_2$ -type (annealed at 1300 °C for 3 hr)  $Y_{2-x}Eu_xSiO_5$  ( $x=0.1$ ) nanoparticles.

morphology and size of the particles by changing the ratio of silicon (TEOS) to yttrium in the precursor solution or the europium doping concentration at a given overall precursor concentration. In general, the particles are spherical in shape, nonagglomerated, and have a narrow size distribution. The mean particle size decreases with the decrease of the overall precursor concentration. For the particles prepared from the precursor solution of  $\phi = 1.25$  and  $x = 0.1$ , the average diameter reduces from 237 nm for the 0.01 M solution (Fig. 2a) to 136 nm for the 0.001 M (Fig. 2b).

The photoluminescence (PL) spectra of the  $X_1$ - and  $X_2$ - $Y_2SiO_5:Eu^{3+}$  particles excited at 254 nm is shown in Fig. 3. For both types of particles, all the intense fluorescence peaks originate in the  $^5D_0$  state of  $Eu^{3+}$  and the strongest one is the hypersensitive electric dipole transition  $^5D_0 \rightarrow ^7F_2$ . However, the spectral character and intensities of the two types of host lattices exhibit clear differences. In  $X_1$ -

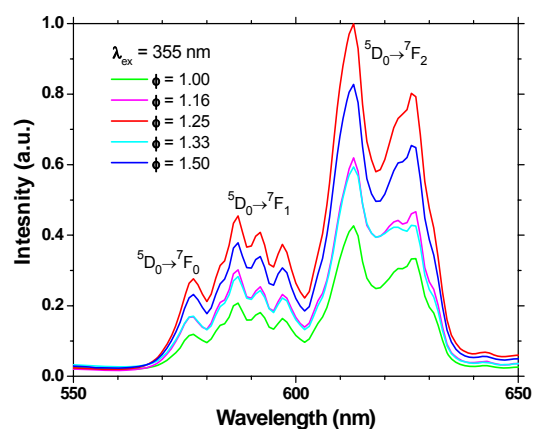


Figure 4: PL spectra of  $X_1$ - $Y_{2-x}Eu_xSiO_5$  ( $x = 0.1$ ) particles from different TEOS concentration.

$Y_2SiO_5:Eu^{3+}$ , the emission spectrum of  $Eu^{3+}$  shows one  $^5D_0 \rightarrow ^7F_0$  peak (577 nm), four  $^5D_0 \rightarrow ^7F_1$  peaks (583, 587, 592, 597 nm), and five  $^5D_0 \rightarrow ^7F_2$  peaks (606, 613, 623, 627, 631 nm), while in  $X_2$ - $Y_2SiO_5:Eu^{3+}$  there's only one  $^5D_0 \rightarrow ^7F_0$  peak (579 nm), three  $^5D_0 \rightarrow ^7F_1$  peaks (587, 594, 596 nm), and four  $^5D_0 \rightarrow ^7F_2$  peaks (611, 618, 622, 626 nm). The integral intensity of  $X_1$  is weaker than that of  $X_2$  and the spectral lines of  $X_1$  is broader than those in  $X_2$ -type.

Figure 4 shows the PL spectra of the  $X_1$ - $Y_{2-x}Eu_xSiO_5$  ( $x = 0.1$ ) particles prepared from different ratios of silicon (TEOS) to yttrium. The excitation wavelength was 355 nm and the overall precursor concentration is 0.1 M for all the cases. For the particles prepared at different silicon equivalence ratios, the spectra characters (i.e. the peak numbers and locations) are almost the same, however, the PL intensities of are strongly affected by the silicon (TEOS) concentration. The maximum PL intensity occurred at an equivalence ratio  $\phi = 1.25$ , and was more than twice the intensity measured in particles prepared from the stoichiometric solution.

Figure 5 shows the PL spectra of particles prepared at different Eu doping concentration. The emission intensity of the  $Y_{2-x}Eu_xSiO_5$  particles was strongly affected by Eu doping concentration. Optimum brightness was obtained at a doping concentration of 30 mol % Eu to yttrium, which corresponds to  $x = 0.6$  in the formula of  $Y_{2-x}Eu_xSiO_5$ . This value is larger than  $x = 0.2$  of bulk materials which have a larger crystalline size [18]. The present result is in good agreement with that of Zhang et al. [11] who reported the quenching concentration of  $x = 0.6$  for sol-gel prepared nanocrystalline  $X_1$ - $Y_2SiO_5:Eu^{3+}$ . For europium doped phosphors, the quenching process is attributed to the energy migration among the activators ( $Eu^{3+}$  ions) which bring excitation energy to the nearby quenching centers (traps). These traps are usually trace impurities or defects on the particle. For bulk  $Y_2SiO_5:Eu^{3+}$  materials, when the Eu doping concentration is low, the luminescent centers are isolated and only a few will transfer energy to the nearby traps. As the Eu concentration increases to  $x = 0.2$ , the luminescent centers become near enough to each other in

the crystal and energy can be rapidly transferred to a trap [11]. As a result, most excited centers lose energy non-radiatively and thus concentration quenching occurs. On the other hand, in  $\text{Y}_2\text{SiO}_5\text{:Eu}^{3+}$  nanoparticles there are only a few traps that are randomly distributed in a particle due to the limited number of primitive cells. As the Eu concentration increases, quenching occurs first in particles containing many traps, while those particles containing few or no traps quench at only high concentration. Consequently, concentration quenching occurs at higher Eu concentrations in nanosized  $\text{Y}_2\text{SiO}_5\text{:Eu}^{3+}$  particles than in bulk ones. The PL intensity of the nanoparticles with high Eu doping concentration is stronger than that of commercial products [12], which suggest new opportunity and potential applications in lamps, displays and other areas.

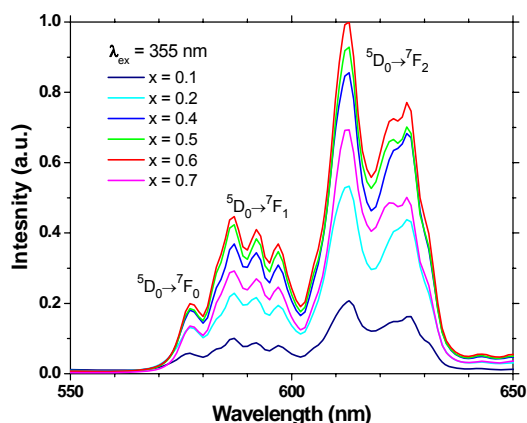


Figure 5: PL spectra of  $\text{X}_1\text{-Y}_{2-x}\text{Eu}_x\text{SiO}_5$  ( $\phi = 1.25$ ) nanophosphors at different Eu doping concentration.

## 4 CONCLUSIONS

$\text{Y}_2\text{SiO}_5\text{:Eu}^{3+}$  nanophosphors were successfully synthesized for the first time by using the flame spray pyrolysis method at various concentrations of precursor solutions. The as-prepared  $\text{Y}_2\text{SiO}_5\text{:Eu}^{3+}$  phosphors exhibit good red luminescence with spherical morphology, narrow size distribution. It was found that the crystal structure and PL intensity of the as-prepared phosphors were strongly affected by the ratio of silicon to yttrium in the precursor solution. Depending on the silicon (TEOS) concentration, the experiment demonstrated that there existed three different crystal phases: an incomplete phase at low TEOS concentrations, a pure phase at intermediate TEOS concentrations, and a  $\text{SiO}_2$  amorphous structure dominated phase at high TEOS concentrations. The  $\text{X}_1$ -type  $\text{Y}_2\text{SiO}_5\text{:Eu}^{3+}$  with pure crystal phase can only be obtained when the silicon concentration was increased to 125% of the stoichiometric precursor solution. It was also shown that the maximum PL intensity occurs at a TEOS equivalence ratio of 1.25. Moreover, a concentration quenching limit was observed at a doping concentration of 30 mol% Eu of yttrium, which corresponds to  $x = 0.6$  in the formula of  $\text{Y}_{2-x}\text{Eu}_x\text{SiO}_5$ . The result suggests that the addition of Si in

$\text{Y}_2\text{O}_3\text{:Eu}^{3+}$  may extend the quenching limit. In addition, the experiment showed that after annealing the  $\text{X}_1\text{-Y}_2\text{SiO}_5\text{:Eu}^{3+}$  particles at 1300 °C, well-crystallized  $\text{X}_2$ -type  $\text{Y}_2\text{SiO}_5\text{:Eu}^{3+}$  phosphors with stronger PL intensity were obtained. The present work demonstrated the advantages of flame spray pyrolysis method for the preparation of  $\text{Y}_2\text{SiO}_5\text{:Eu}^{3+}$  nanophosphors and the potential for industrial applications.

## REFERENCES

- [1] Shmulovich J, Berkstresser G W, Brandle C D and Valentino A 1988 Single-crystal rare-earth-doped yttrium orthosilicate phosphors *J. Electrochem. Soc.*, **135** 3141.
- [2] Li C, Wyon C and Moncorge R 1992 Spectroscopic properties and fluorescence dynamics of  $\text{Er}^{3+}$  and  $\text{Yb}^{3+}$  in  $\text{Y}_2\text{SiO}_5$  *IEEE J. Quantum Electron.* **28** 1209.
- [3] Jacquemet M, Balembois F, Chenais S, Druon F, Georges P, Gaume R and Ferrand B 2004 First diode-pumped Yb-doped solid-state laser continuously tunable between 1000 and 1010 nm *Appl. Phys. B* **78** 13.
- [4] Peters T E 1969 Cathodoluminescent  $\text{Ln}_y(\text{SiO}_2)_x\text{-Tb}$  phosphors *J. Electrochem. Soc.*, **116** 985.
- [5] Kang Y C, Lenggono I W, Park S B and Okuyama K 1999  $\text{Y}_2\text{SiO}_5\text{:Ce}$  phosphor particles 0.5-1.4  $\mu\text{m}$  in size with spherical morphology *J. Solid State Chem.* **146** 168.
- [6] Ouyang X, Kitai A H and Siegle R 1995 Rare-earth-doped transparent yttrium silicate thin-film phosphors for color displays *Thin Solid Films* **254** 268.
- [7] Mitsunaga M, Yano R and Uesugi N 1991 Time-domain and frequency-domain hybrid optical memory – 1.6 kbit data-storage in  $\text{Eu}^{3+}\text{-Y}_2\text{SiO}_5$  *Opt. Lett.* **16** 1890.
- [8] Ito J and Johnson H 1968 Synthesis and study of yttrialite *Am. Miner.* **53** 1940.
- [9] Taghavinia N, Lerondel G, Makino H and Yao T 2004 Europium-doped yttrium silicate nanoparticles embedded in a porous  $\text{SiO}_2$  matrix *Nanotechnology* **15** 549.
- [10] Yin M, Zhang W, Xia S and Krupa J C 1996 Luminescence of nanometric scale  $\text{Y}_2\text{SiO}_5\text{:Eu}^{3+}$  *J. Lumin.* **68** 335.
- [11] Zhang W, Xie P, Duan C, Yan K, Yin M, Lou L, Xia S and Krupa J C 1998 Preparation and size effect on concentration quenching of nanocrystalline *Chem. Phys. Letters* **292** 133.
- [12] Duan C-K, Yin M, Yan K and Reid M F 2000 Surface and size effects and energy transfer phenomenon on the luminescence of nanocrystalline  $\text{X}_1\text{-Y}_2\text{SiO}_5\text{:Eu}^{3+}$  *J. Alloys Compd.* **303-305** 371.
- [13] Huang H and Yan B 2004 In situ sol-gel composition of multicomponent hybrid precursors to luminescent novel unexpected microrod of  $\text{Y}_2\text{SiO}_5\text{:Eu}^{3+}$  employing different silicate sources *Solid State Comm.* **132** 773.
- [14] Kang H S, Kang Y C, Park H D and Shul Y G 2005  $\text{Y}_2\text{SiO}_5\text{:Tb}$  phosphor particles prepared from colloidal and aqueous solutions by spray pyrolysis *Appl. Phys. A* **80** 347.
- [15] Qin X, Ju Y, Bernhard S and Yao N 2005 Flame synthesis of  $\text{Y}_2\text{O}_3\text{:Eu}$  nanophosphors using ethanol as precursor solvents *J. Mater. Res.* in press.
- [16] Joint Committee on Powder Diffraction Standards (ASTM), PDF Card No. 21-1456.
- [17] Joint Committee on Powder Diffraction Standards (ASTM), PDF Card No. 21-1458.
- [18] Holsa J, Jyrkas K and Leskela M 1986 *J. Less-Common Met.* **126** 215.